Multimodal Minimally Invasive Wearable Technology for Epilepsy Monitoring: A Feasibility Study of the Periauricular Area

Guillermo M. Besné Villanueva, Peio Lopez-Iturri, Manuel Alegre Esteban, Julio Artieda González Granda, Jesús D. Trigo, Luis Serrano-Arriezu, *Senior Member, IEEE*, Francisco Falcone, *Senior Member, IEEE*, and Miguel Valencia Ustarroz

***Abstract*—Ambulatory monitoring is of great interest in both clinical and domestic environments. Despite the technological advances, few monitoring solutions are suitable for medical application and diagnosis. Here, we investigate the feasibility of targeting the periauricular area (ear pavilion, ear canal, and the surrounding skin areas) to implement a multimodal system that fulfills the requirements of ergonomics and minimal obstructiveness in the context of epilepsy monitoring. Six physiological signals are selected and explored for their integration in the area of interest and a "proof-of-concept" prototype integrating the components in a single portable device targeting the selected location is implemented. Results show mixed results where some parameters are highly reliable, and others are impractical or require customized technology to provide clinically relevant information. To enable data acquisition, storage, and processing within the Internet of Medical Things paradigms, wireless body area transceiver integration is also analyzed in terms of coverage/capacity relations, showing feasibility for such device configuration.**

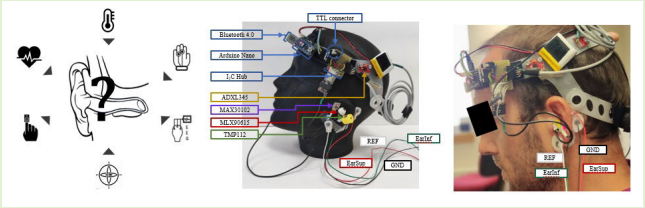

***Index Terms*— Ambulatory monitoring, epilepsy, multimodal wearable, periauricular area.**

I. Introduction

THE chronification of some diseases and the increase in technological knowledge by the general population results on a higher number of medical experts, patients, and relatives demanding a better use of technological innovations. Their claim is to ensure accurate diagnosis and provide continuous monitoring and personalized treatments [1], [2], [3], [4], [5].

In recent years, technological advances have made it possible to implement increasingly versatile sensors, smaller in size and with lower consumption. These developments, together with the possibility of transmitting, processing, and storing a large amount of information, might represent a shift of paradigm in the way we understand and use "data" for disease management. Technology has improved consumer electronics leading to a surge of wearable devices capable of monitoring physiological parameters, such as hear rate, calories consumption, physical exercise intensity, or estimates of sleep stages. However, very few of these solutions are suitable for medical application and diagnosis [6]. This might be explained by the fact that the process of adopting some technological solution for monitoring diseases is not easy [7], [8], [9], [10]. Leaving aside concepts, such as privacy and clinical data security, their success lies in the ability to implement features such as: 1) portability; 2) ease of use; 3) robustness; 4) precision (compared to those provided by clinical and specialized settings); and 5) coverage of parameters to provide (clinically) relevant information. In addition, and depending on

Manuscript received 28 August 2023; accepted 6 September 2023. Date of publication 18 September 2023; date of current version 31 October 2023. This work was supported in part by the Department of Economic Development of the Government of Navarra under Grant GN 2019 PC078-079; in part by the Carlos III Health Institute through the project under Grant DTS19/00130 (co-financed by the European Regional Development Fund; "A way to make Europe"); and in part by the Agencia Estatal de Investigación, Fondo Europeo de Desarrollo Regional -FEDER-, European Union under Grant PID2021-127409OB-C31 CONDOR. The work of Guillermo M. Besné Villanueva was supported by the "Asociación de Amigos de la Universidad de Navarra, ADA" during his Ph.D. The associate editor coordinating the review of this article and approving it for publication was Dr. Edward Sazonov. *(Corresponding author: Miguel Valencia Ustarroz.)*

This work involved human subjects or animals in its research. Approval of all ethical and experimental procedures and protocols was granted by the Local Ethical Committee of the University of Navarra under Approval No. CEIC-2021.143.

Please see the Acknowledgment section of this article for the author affiliations.

Digital Object Identifier 10.1109/JSEN.2023.3314190

the disease or monitoring circumstances, it is necessary to identify, among others, the most suitable variables of interest, location/optimization of the sensitization points, degree of miniaturization, level of obstruction, anatomic constraints, or ergonomics needs.

Continuous monitoring and personalized follow-up is of high interest in diseases, such as epilepsy: a chronic neurologic condition marked by the recurrence of unprovoked seizures [11], [12]. Seizures are paroxysmal events that result from abnormal neuronal discharges and manifest in the form of sudden, stereotyped episodes with accompanying changes in motor activity, sensation, and behavior, thus exposing the patient to life-threatening situations [13], [14]. Seizures result in increased injuries and mortality, including sudden unexpected death in epilepsy (SUDEP). This scenario makes constant supervision a requirement, even during night [15], [16]. The need of chronic intake of antiepileptic drugs (AEDs) also leads to potential side effects that require continuous adjustment of the treatment. Despite handwritten diaries where patients' evolution is reflected, disease perception and patients' mood have drastic effects on reports to neurologists and neuropediatricians. Consequently, unnecessary or even inadequate treatment adjustments are frequent [17].

All these scenarios justify the need for monitoring systems suitable for their operation on domestic or ambulatory environments. Ideally, such developments should implement multimodal, minimally obstructive monitoring systems capable to provide information clinically relevant to assess the physiological and neurological state of the subject. As critical as the parameters to measure, it is also important to identify an appropriate recording location. All parameters selected must be susceptible to be measured, with little or nonintrusive approximation, complying with structural stability capable of supporting robust and prolonged monitoring periods of time. The periauricular area (the external ear, the ear canal, and the surrounding skin area) seems to be a good candidate; the anatomical location and rigidity of the ear canal provide great support to anchor potential devices, such as earphones or hearing aids with low stigmatization. In addition, previous reports have described the possibility of obtaining reliable, long term, and clinically relevant measures of different biosignals. Nevertheless, combining several signal modalities in one single setup represents a big challenge and requires the systematic assessment of their feasibility when being recorded at the same time.

In the case of epilepsy patients, a number of such physiological measurements can be of special relevance; parameters, such as electroencephalogram (EEG), acceleration (Acc), electrocardiogram (ECG), peripheral oximetry (SpO_2), body core temperature (T^a), and galvanic skin response (GSR), could provide an integral assessment of the general state of the patient.

The EEG is the register of electrical activity generated by the brain [18], [19]. In the case of epilepsy, the EEG represents one of the most important tools for diagnosis and follow-up. In epileptic patients both during seizures and interictal periods, the brain generates abnormal activities easily identified in the EEG traces. In this context, EEG recordings in the ear canal have been introduced recently [20] resulting in different implementations that also include wireless capabilities [21], [22], [23], [24], [25]. In the area of interest, the EEG can be recorded through electrodes located within the ear canal (in-earEEG) or disposed around the ear pavilion and provide relevant information for the detection of seizures in patients with focal and generalized epilepsies [26], [27].

Acceleration represents a straightforward method to quantify the amount of movement. Measurements can refer to dynamic acceleration, where speed changes of the monitored object are quantified; or static acceleration with measurements are due to gravity, thus making it possible to estimate the object's orientation relative to Earth's surface. In the case of epilepsy, acceleration has been successfully integrated into warning systems to detect seizures [28], [29]. In addition, it can be used for fall detection and head orientation assessment [30], to quantify the amount of movement and identify postural changes or the presence of abnormal movements [31]. As for placement, the acceleration measurement of the head is less restrictive with its placement. As a rigid body, the movement of the head can be monitored at any point, including the periauricular area.

ECG records electrical activity from the heart myocardium [32]. Polarization and depolarization sequences leading to heart contraction result in a series of waveforms that can be divided into P-wave, QRS complex, and T-wave. To obtain a high-quality ECG suitable for cardiovascular diagnosis, a set of nine electrodes are required [33]. However, for simpler approaches, such as those aimed at estimating the heart rate (HR) or their variations in time [heartrate variability (HRV)], three or even two electrodes are sufficient. Variations on the HR are used as surrogates of distress at multiple levels; in the context of epilepsy, they have proved to be useful to detect the occurrence and onset of epileptic seizures [34], [35], [36], and SUDEP events. Nevertheless, and in the case of periauricular area (under the constraint of unique and unilateral placement of the electrodes), the geometry of the heart versus (one) ear could present some difficulties to provide reliable ECG measurements.

Photoplethysmography (PPG) measures volumetric variations of blood circulation though optical inexpensive methods. By using different light sources and photodetectors at the surface of skin, PPG allows to estimate HR, oxygen saturation in peripheral blood (SpO_2), and other parameters suitable for assessing the state of the cardiovascular system [37], [38]. Green light (530 nm) sources are optimal to determine the HR on continuous monitoring setups as it is more sensible to small volume changes and results more robust against movement artifacts [39]. Complementarily, red (650 nm) and infrared (IR, 940 nm) sources are used to exploit absorption differences of hemoglobin on its reduced (Hb) and oxygenized (HbO2) state and permit to extract SpO_2 [40]. In the context of epilepsy, PPG can serve to estimate HR and HRV as an alternative to ECG measures. It allows to study cardiorespiratory coupling changes and SpO_2 levels can be useful to predict/detect epileptic seizures, although it might be problematic to implement for tonic–clonic seizures [41], [42], [43]. Common placements for PPG sensors include the earlobe that it is highly irrigated. Fingers are the most usual, but other implementations with custom PPG sensors on in-ear devices have been built and performed satisfactorily

acquiring the PPG signal on the concha or in the ear canal [44].

As endothermic animal, humans can generate their own body temperature by means of metabolic rate, sweating, vasoconstriction, and other physiological mechanism. The most common alteration in temperature is fever, an abnormal rise on core body temperature. The ability of thermoregulation and being able to withstand external temperature varies at different ages. Adults have larger bodies and greater volume-to-surface ratio, and therefore, a higher resistance to external temperatures affects their core body temperature. As such, children are more susceptible to suffering hyperthermia and hypothermia under the same circumstances [45]. Given this condition, febrile seizures are more common among children, making body temperature a critical parameter. This measurement is even more critical among for some specific epileptic patients, as they are far more sensitive to temperature changes and frequently trigger seizures [46]. Measuring core body temperature, more reliable than peripheral temperature, requires placing sensors in specific locations [47]. The tympanum is one of the best areas to estimate the core temperature along with the anus or the armpit. Nevertheless, its applicability is far more convenient and suitable for sustained monitoring.

GSR, also known as electrodermal activity (EDA), measures the conductance or resistance of the skin. GSA is directly related to sweat gland activity that is regulated by sympathetic and parasympathetic nervous systems [48], [49]. Arousal of emotional, sensorial, or physiological origin modulates the balance between these two systems and modifies skin conductance [50]. Application for epilepsy patients include stress-level assessment that could serve to prevent the onset of certain types of seizures; paired with accelerometers, it is used to detect convulsive seizures [51] and SUDEP [52]. Previous works performed GSR measurements on multiple areas to confirm their validity [53]. Among them, the closest one to the desired area is the neck: placing the electrodes on the nape on both sides of the spine. These works combined with the population of sweat glands on both areas could allow GSR acquisition on this area [54].

Here, we explore the feasibility of integration of these six selected measures in the periauricular area. Several efforts have succeeded in implementing unimodal devices providing a unique physiological modality of recording. Others have proposed the combination of multiple devices to increase the number of parameters measured, but at the cost of increasing complexity (using several recording points across the body) and decreasing ergonomics and ease of use. Integrating all these measurements in a single device opens the possibility to implement a multimodal monitoring system, minimally obstructive, and ergonomic, with the capability to gather information that could be crucial in the diagnosis and follow-up of patients, including the capability of providing an SUDEP and seizure warning system, but attending to principles of ergonomics, robustness, and reliability.

Finally, and to enable the inclusion of the monitoring platform within medical health systems following the paradigms of smart health and the Internet of Medical Things (IoMT), the integration of communication system appears as a key factor in the development of such multimodal monitoring system. The proposed approach, taking advantage of wearable devices, requires user mobility as well to provide high ergonomic levels, leading to the use of wireless communication technologies. Among these, body area network (BAN) protocols are widely employed, due to low form factor, low energy consumption, moderate cost, and transmission rates in the 1–2-Mbps range. In this sense, Bluetooth is commonplace in wearable connectivity, tethering either to other wearable devices such as smart watch and smartphones or to infrastructure gateways, enabling user interaction as well as web/cloud connectivity inherently [63]. The integration of wireless transceivers within the sensor platform is conditioned by the characteristics of radio propagation in BAN scenarios, which can consider on-body, off-body, and in-body communication links. These specific communication links exhibit losses and potential degradation due to different effects, such as body impact (in terms of penetration losses, shadowing, and scattering), human body dynamics, modification of antenna operational characteristics (e.g., operation frequency, bandwidth, input impedance, and radiation diagram), and multipath propagation components from the surrounding environment [64]. Coverage/capacity requirements must be fulfilled to provide adequate quality of service metrics, in terms of bit error, rate/block error, and rate/latency thresholds. Small-scale statistics as well as path loss approximations have been obtained to provide assessment in relation to operational conditions of wireless transceivers operating in BAN configurations [63], [64].

II. Materials and Methods

The feasibility and validity of recording the proposed parameters on the auricular area were performed by first recording each modality individually and finally integrating all of them in a former multimodal recording where a proof-of-principle multimodal system is built. Recordings were performed by ten volunteers. Recording equipment, protocols, and paradigms were approved by the Local Ethical Committee of the University of Navarra (Ref: CEIC-2021.143) following international guidelines. Inclusion criteria for recruited subjects were: 1) age ranging from 20 to 40 years old; 2) no known cardiac; or 3) no neurological disease.

A. Electroencephalography

Feasibility and validity of recording EEG activity in the area of interest were performed according to three different paradigms previously explored [55]. Two electrodes were placed in the periauricular area (above the ear: EarSup and below the ear: EarInf). As a gold standard, the activity of a third electrode on the occipital region (Oz position following the 10:20 system) was also recorded. All the three electrodes were referred to the earlobe and the ground electrode was placed on the mastoid. EEG recordings were performed by using BrainAmp EEG amplifiers (BrainProducts, https://brainvision.com/) connected with an STIM2 system (Compumedics Neuroscan, https://compumedicsneuroscan.com/product/stim2-precise-stimulus-presentation/) to deliver visual stimuli.

Under the α-band modulation paradigm, volunteers were placed in a relaxed position, wake while keeping the eyes open for 30 s. Afterward, they closed their eyes (without falling asleep) for another 30 s. This was repeated at least ten several times, modulating brain's waves, and an increase in the brain activity on the α band (8–12 Hz) is observed. This modulation is compared between recording areas by performing a power spectrum density (PSD) [56], [57] for each state and then quantifying the modulation on the α-band and the exact frequency of the peak.

Then, we recorded visual evoked potentials (VEPs): on a relaxed position, volunteers were stimulated visually by means of an alternating chessboard pattern that changed every 1.1667 s (∼0.854 Hz). The alternating pattern stimulates the visual system and elicits prototypic brain responses locked to the stimulus that show a series of positive and negative peaks at very specific latencies [58]. Accordingly, we determined the feasibility of obtaining such responses on the selected area and compared their latencies with those recorded over the occipital area.

Finally, we evaluated the visual steady-state responses (VSSRs) on the periauricular region. To do that, we used the same chessboard stimulus but increasing the frequency to 8.54 Hz. Responses were obtained by performing a PSD for each area and comparing the power and frequency of the main response.

B. Acceleration

Acceleration measurements were performed with the triaxial linear accelerometer ADXL345 (Analog Devices, https://www.analog.com/en/products/adxl345.html). During the recordings, the accelerometer was firmly attached to the side of the head close to the ear and volunteers perform three different sets of movements: postural changes (roll, pitch, and yaw), walking, and jumping.

To minimize the potential effects of the interindividual differences both in the orientation of the sensor and in the dynamics of the performed activities (e.g., velocities in the execution of the jumping phase), a rotation on the *XYZ*-axis of accelerometer followed by a dynamic time warping (DTW) [59], [60] of the signals was computed. By doing so, we were able to align the different time series across paradigms and subjects.

C. Cardiovascular Monitoring

For this experiment, two modalities are ECG and PPG. In our experiments, we used a BiosignalsPlux Explorer system from Plux Biosignals (https://plux.info/34-kits) and an Arduino-based fully integrated system for physiological research. We evaluated several configurations: 1) chest ECG as gold standard (following Plux indications); 2) ear ECG; 3) PPG on the fingertip as gold standard; and 4) PPG on the ear canal. To place the PPG sensor on the ear canal and generate some pressure against the tissue, the PPG sensor was embedded in a viscoelastic earplug.

From the ECG, we detected heartbeats and estimated the HR. Then, the Bland–Altman [61] analysis was used to compare the HR estimated from the chest ECG with those obtained from the ear ECG, finger PPG, and ear PPG.

Next, we explored the possibility to integrate the MAX-30102 PPG sensor (https://www.maximintegrated.com/en/products/interface/sensor-interface/MAX30102.html), which provides capabilities to provide SpO_2 information. Recordings were performed on the following locations: two gold standard areas: fingertip and ear lobe; and two alternative areas: the ear canal and behind the ear (over the mastoid process).

D. Body Temperature

For body temperature assessment, the MLX90615 IR temperature sensor (https://www.melexis.com/en/product/MLX90615) and the TMP112 thermocouple (https://www.ti.com/product/TMP112) were explored. The MLX90615 is a low power consumption IR temperature sensor with 0.5 °C of precision and 0.02 °C of resolution. Despite its small dimensions, it could be problematic for our aim, as it would obstruct completely the ear canal, preventing any aeration and obstructing sound from reaching to the tympanum. TMP112 is a miniaturized thermocouple-based sensor (1.6 × 1.6 mm), with low consumption, 0.5 °C accuracy, and 0.0625 °C resolution. Complimentarily, we also explored the possibility to use the temperature sensor integrated into the MAX30102 PPG (used to internally calibrate the IR readings of the PPG photodiode). Nevertheless, although MAX30102 would be the best choice in terms of potential integration, it has the lowest precision (1 °C).

To assess the suitability of these sensors for future implementations, we obtained their calibration curves. To do that, sensors were faced to a hot body and the temperature was measured as the temperature dropped gradually; a commercial IR thermometer Thermoval Baby was used as a reference. Then, we evaluated the capability of the sensors to follow changes in the temperature; sensors went through three temperature stages: 1) room temperature (around 20 °C) for 30 min; 2) cold room (around 2 °C) for 60 min; and 3) room temperature for another 30 min.

From these analyses, we selected the TMP102 thermocouple and proceeded with recording on the volunteers. The TMP102 was embedded in a viscoelastic earplug and inserted in the ear canal, and subjects were asked to move across several rooms with different temperatures: 2 min in an office (room temperature ∼20 °C), 2 min in a ∼5 °C refrigerated room, 1 min in a ∼−15 °C refrigerated room, again back for 2 min at the ∼5 °C room, and finally 2 min in the office. The exact room temperature was recorded simultaneously with another TMP102 thermocouple.

E. Galvanic Skin Response

The equipment used for GSR validation was again the BiosignalsPlux Explorer with the EDA (electrodermal activity, equivalent to GSR) sensor. To modulate their autonomic response, volunteers were asked to watch 6-min-long recompilation of short suspense videos and then asked to perform six consecutive Valsalva maneuvers. GSR sensors are placed between: 1) index and middle finger as gold standard and

2) the tragus and the mastoid process ipsilaterally to the previous configuration. After visual inspection of the recorded data, analysis on the influence of the maneuvers was determined on frequency bands: 0.1–0.2, 0.2–0.3, 0.3–0.4, and 0.4–1.0 Hz [62].

F. Proof-of-Concept Prototype

Finally, and with a selection of the most suitable components, we proceeded with their integration in a prototype considering factors of: 1) modularity; 2) wearability; 3) reliability; and 4) ease of use. This prototype is designed as a "proof of concept" to test the possibility of performing a simultaneous multimodal recoding of the selected variables together with the ability of a simple microcontroller, such as an Arduino Nano, to manage the components and broadcast the recorded signals through wireless technology. Although in terms of miniaturization, placement, and degree of integration, the microcontroller specifications were not considered key in this stage of the development, attention was focused on the dimensions and placement of the sensors, which were considered critical to fulfill with the volumetric restrictions imposed by the area of interest (they must be small enough to fit inside or around the ear canal of volunteers).

G. Body Area Network Wireless Connectivity

Different BAN topologies have been considered, employing Bluetooth classic and Bluetooth Low Energy (BLE) systems following the path loss methodology described in [64], which considers the receiver position at chest or hip and the transmitter positions at chest, back, right wrist, and left wrist. Different transceiver operation conditions have been considered, in terms of parameters such as use of frequency hopping, transmission power setting, or receiver sensitivity thresholds. Further insight is obtained by performing full-wave electromagnetic analysis of wireless intrabody propagation links. These results will be further discussed in the following section.

III. Results

In this section, the results of the feasibility studies for each individual modality are exemplified by showing the data from a representative subject. Then, a quantitative analysis, including all ten subjects, is presented. For the proof-of-concept prototype, an implementation example with a representative recording is provided. Finally, wireless connectivity modeling results for a BAN are shown.

A. Electroencephalography

Fig. 1 shows the effect of closing the eyes on the modulation of the alpha oscillations for the Oz, EarSup, and EarInf locations. Although the amplitude over Oz is larger than that recorded in the ear areas, the analysis of the prominence of the peaks confirms the existence of a significant modulation of the amplitude (but not the frequency) of the alpha rhythm all over the three locations (see Fig. 2).

For the VEPs, the results confirm that the maximal response is detected at Oz; nevertheless, latencies for N75, P100, and

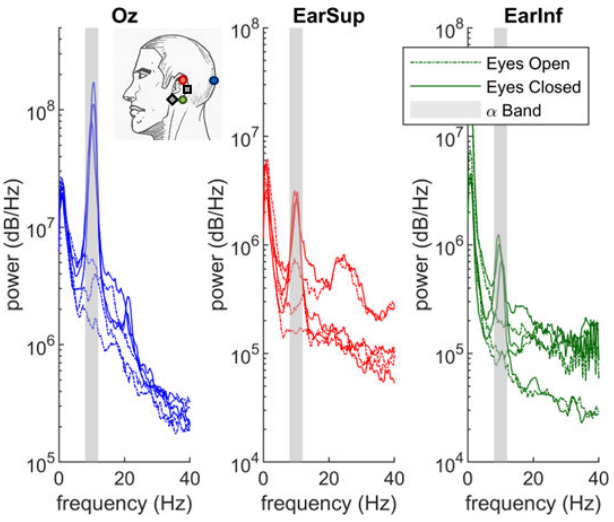

Fig. 1. Power spectrum of the acquired signal during the α-attenuation study of three representative subjects. Continuous lines correspond to the eyes-closed condition and dotted lines to the eyes-open period on the corresponding areas: occipital, above the ear, and below the ear (left to right).

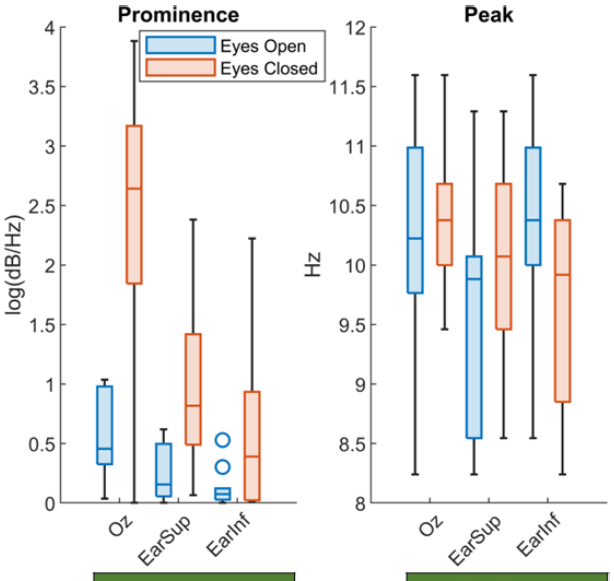

		Prominence		
		Oz	EarSup	EarInf
Open	Mean	0.54	0.25	0.13
	SD	0.36	0.23	0.17
Closed	Mean	2.29	0.97	0.64
	SD	1.20	0.66	0.74
Significance		<0.001	0.006	0.04

		Prominence		
		Oz	EarSup	EarInf
Open	Mean	0.54	0.25	0.13
	STD	0.36	0.23	0.17
Closed	Mean	2.29	0.97	0.64
	STD	1.20	0.66	0.74
Significance		***	**	*

Fig. 2. Study of prominence and frequency of the alpha rhythm modulation during the closed–open eyes study.

N140 are maintained across the three locations, showing no significant differences, thus demonstrating that despite the lower amplitude of the responses, it is possible to obtain VEP responses in the periauricular area (see Fig. 3).

As for the case of the VEPs, the VSSR were also detected on the three selected recording areas. Fig. 4 shows the VSSR response from a representative subject together with the

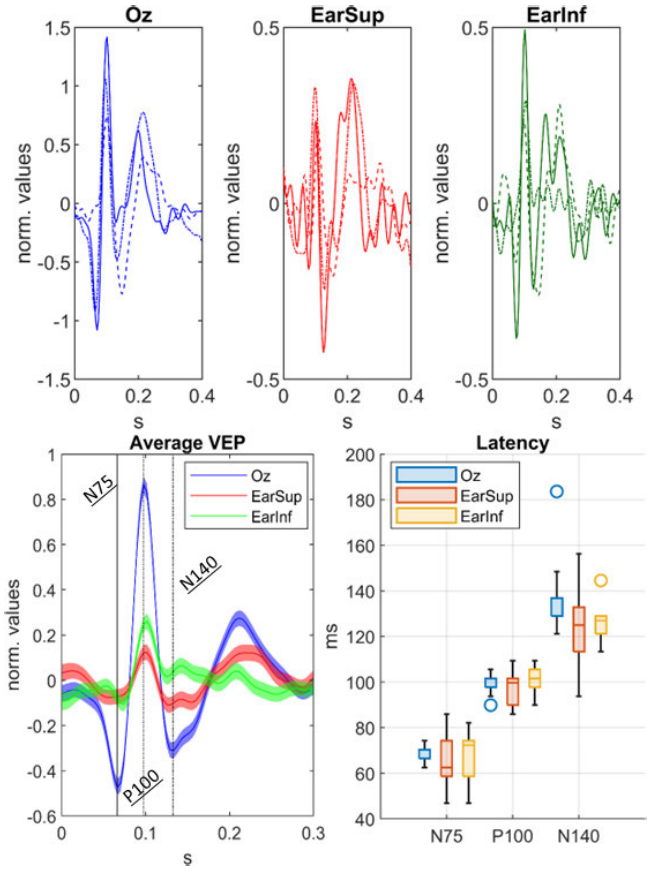

Fig. 3. VEP waveforms corresponding to three representative subjects on the corresponding areas (occipital, above the ear, and below the ear; top panel from left to right). Average VEP for all volunteers at each recording location (bottom panel, left) and box-plot representation of the latencies of the N75, P100, and N140 peaks (bottom panel, right).

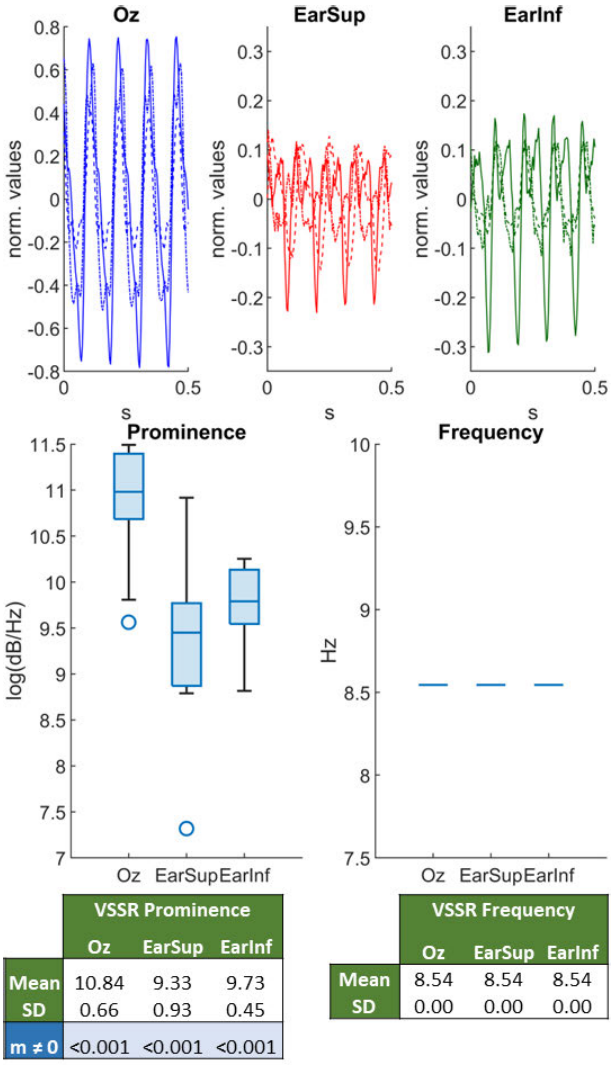

VSSR Prominence	Oz	EarSup	EarInf
Mean	10.84	9.33	9.73
SD	0.66	0.93	0.45
m ≠ 0	<0.001	<0.001	<0.001

VSSR Frequency	Oz	EarSup	EarInf
Mean	8.54	8.54	8.54
SD	0.00	0.00	0.00

Fig. 4. VSSR of three representative subjects at the three selected locations together with the analyses of the prominence and frequency of such responses for the ten volunteers involved in the study.

analysis of the amplitude and frequency of the responses for the ten subjects. Results show that although maximal responses are detected at Oz, it is possible to record VSSR in the periauricular area with a good SNR for their detection and with no deviation of the frequency (that is expected to be 8.54 Hz).

B. Acceleration

Fig. 5 shows a 3-D representation of the linear acceleration recorded for all subjects. After a coordinate axis rotation (see methods), trajectories show a good concordance between subjects and differences between the three different movements tested (postural changes, walking, and jumping). Indeed, a simple correlation analysis (see Fig. 6) suggests the suitability of these measures to implement a detection algorithm to identify them. Finally, it is worth noting that the information provided by the static acceleration also allows differentiating between postures within the postural changes test.

C. Cardiovascular Monitoring

Fig. 7 shows ECG recordings together with the detected heartbeats for the three different configurations investigated. Visual inspection shows that both chest and head–shoulder recordings show recognizable QRS complexes. In contrast, the recording performed on auricular area does not show recognizable QRS complexes. This makes it difficult to detect the heartbeat and, thus, the estimation of the HR. Indeed, the Bland–Altman analysis of HR estimated from head–shoulder ECG and ear ECG with respect to chest ECG demonstrates that the head–shoulder derivation provides a far better HR estimation of the HR (using chest ECG as gold standard) than that obtained from the auricular area (see Fig. 8 for Bland–Altman plot of a representative subject).

In contrast, HR values derived from PPG signals both from finger and auricular provide good estimates of the HR. Fig. 9 shows an example of a combined chest-ECG and in-ear PPG recording together with Bland–Altman plots that demonstrate that the estimation of the HR from the PPG obtained in both regions is comparable to that obtained from the chest ECG.

Fig. 10 shows an example of the capability of the MAX30102 PPG sensor to provide PPG information and SpO_2 information from the finger and three different points of the periauricular area. For the SpO_2 data, it should be noted:

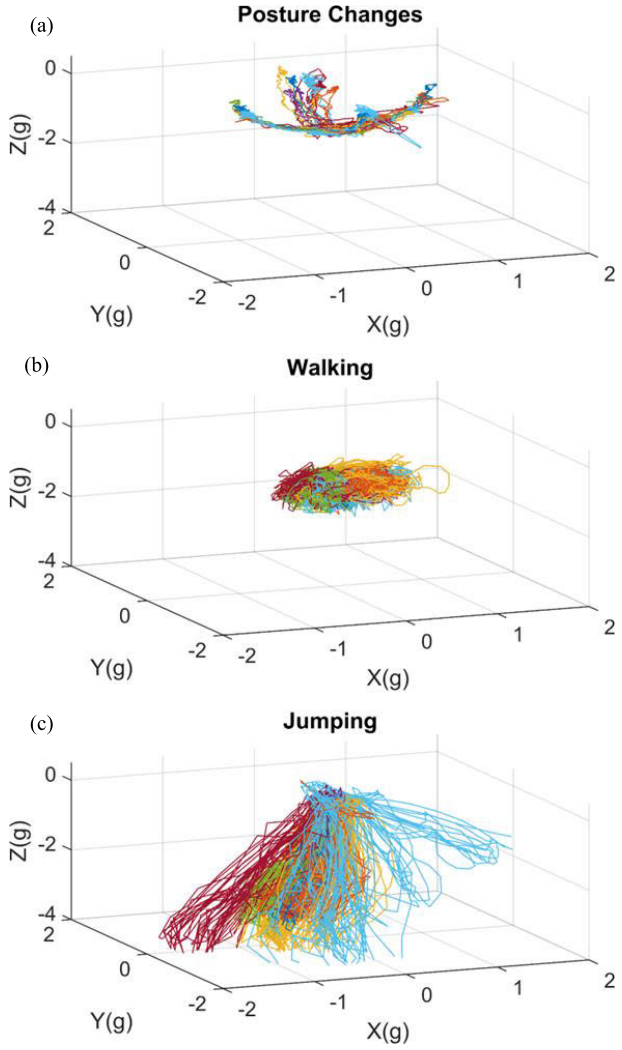

Fig. 5. Triaxial linear acceleration measurements for the ten volunteers under (a) postural changes, (b) walking, and (c) jumping (each color corresponds to each of the subjects).

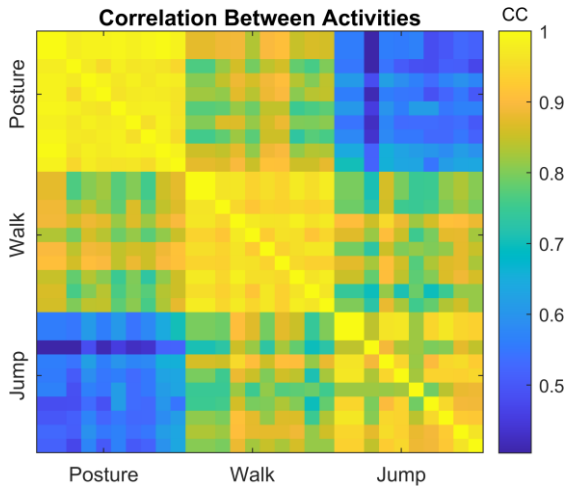

Fig. 6. Correlation values obtained for all recorded activities organized by subject and volunteer.

1) that these are noncalibrated estimates that serve to prove the feasibility of the measurements and 2) that the dimensions of the PCB hosting the PPG sensor difficulties the skin-sensor

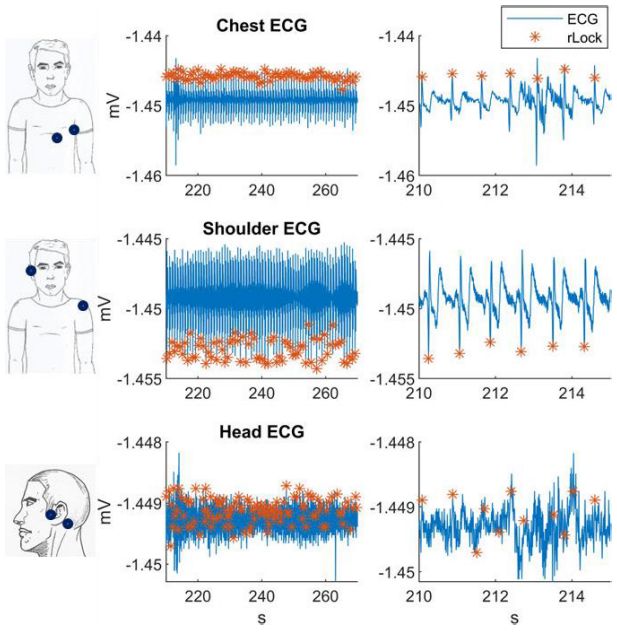

Fig. 7. Raw ECG measured on (a) chest, (b) between the ear and the contralateral shoulder, and (c) auricular area. The body sketches on the left represent the location of the electrodes, the plots on the center 80-s sample recorded on each area, and the plots on the right a 5-s sample of the same signals.

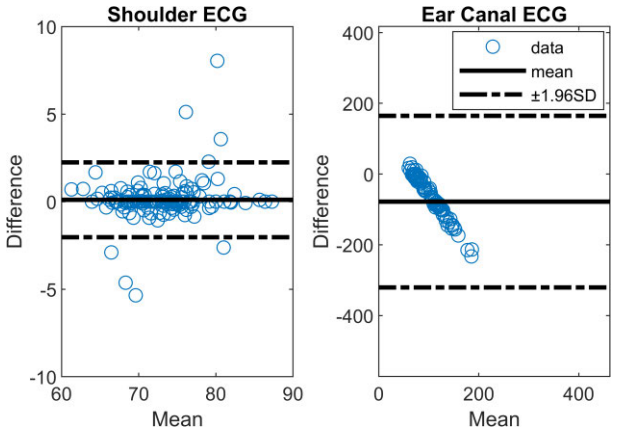

Fig. 8. Bland–Altman representation of the HR obtained from ECG from (a) chest and head–shoulder and (b) chest and auricular area. Please note the difference of scales in the two panels, as panel A scales are [−15, 15] and [55, 100] bpm, and for panel B, they are [−1000, 900] and [0, 1600] bpm.

contact and this causes at some points movement-related artifacts in the SpO_2 estimation.

D. Body Temperature

The comparative analysis of the three temperature sensors showed that the performance of the thermistor integrated in the MAX30102 PPG sensor was the lowest in terms of precision and dynamics of the response to temperature changes. On the other hand, and despite the good performance of the MLX90615 IR temperature, this sensor was not considered as it fully blocks the ear canal, thus precluding the aeration and limiting the sound perception. As a result, we selected the TMP112 to proceed with the validation study on the ten

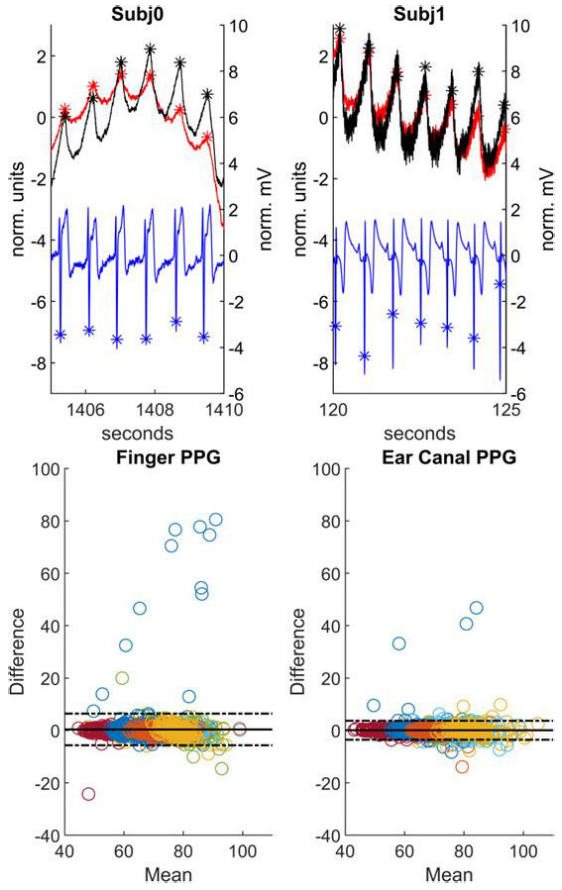

Fig. 9. Top panels: simultaneous chest ECG and in-ear PPG recordings in two representative subjects. Bottom panels: Bland–Altman analysis for all subjects comparing the HR estimation on chest ECG against the finger PPG and auricular area PPG.

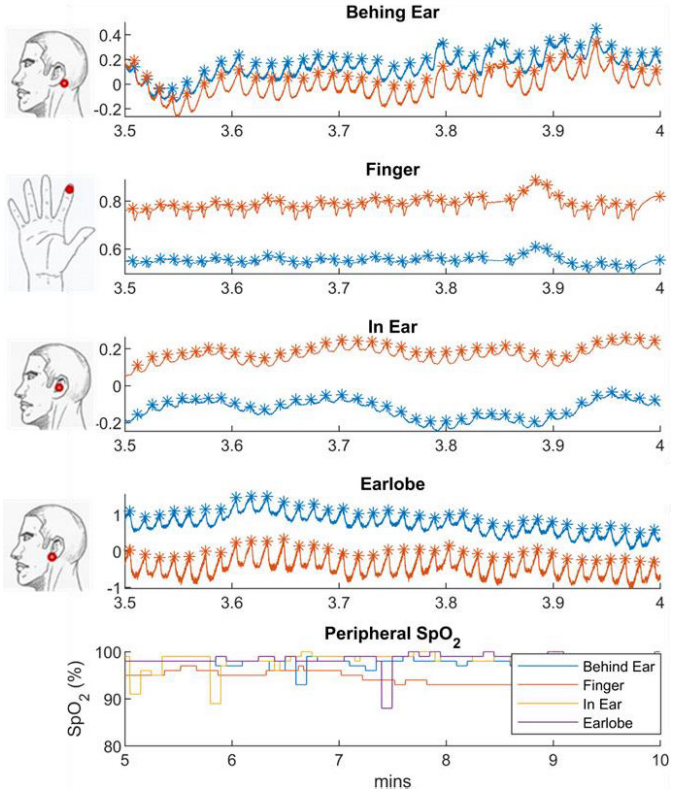

Fig. 10. PPG recordings on all four defined areas where the blue plot represents red LED PPG and orange IR LED PPEG. The dots over each line represent the estimated location of a heartbeat. The exact placement of the sensor is indicated on the picture at the left of each graphic. Bottom panel: SpO_2 estimated from PPG registers on the corresponding PPG recordings. The different levels of each area are due to noncalibrated estimation, and the severe artifacts on in-ear registers are the results of an incompatible form factor of the sensor with ear canal.

volunteers. As shown in Fig. 11, the effect on the temperature measured in the ear canal is barely affected by the changes in the room temperature. In contrast, the ambient sensor shows the effects of moving from room office to cold rooms at -5 °C and -15 °C and back to the office. All these results demonstrate the suitability of measuring the core temperature in the era canal as opposed to the use of wrist-worn sensors.

E. Galvanic Skin Response

The GSR recordings in Fig. 12 illustrate the impossibility of the selected hardware to capture the modulation of the GSR in the periauricular region. Although it is capable to obtain significant (and similar) GSR modulations in both hands, no apparent modulation is observed when placing the electrodes between the tragus and the mastoid. Further statistical analysis on the four selected frequency bands ([0.1, 0.2], [0.2, 0.3], [0.3, 0.4], and [0.4, 1.0] Hz) confirms this observation, both for the Valsalva and video watching conditions (see Fig. 13).

F. Proof-of-Concept Prototype

The results presented above did not only serve the purpose of validating the area for these measurements but also to determine the suitability of the discrete electronic components selected. At this point, we then proceeded with the design and implementation of a "proof-of-concept" prototype aimed at determining the feasibility of a simultaneous recording of the selected measures through a unique microcontroller.

Fig. 14 shows this first prototype integrating: 1) TMP112 thermistor for in-ear temperature measurement; 2) TMP102 for ambient temperature measurement; 3) MLX90615 IR thermometer for contactless tympanic temperature measurement; 4) MAX30102 for PPG recordings; and 5) ADXL345 for acceleration recording. Schematics show the placement of the different components. Both TMP102 and ADXL345 are not placed directly on the periauricular area as the TMP102 is used to measure ambient temperature (thus, it is placed far from the area of recording) and the placement of the accelerometer does not require to be exactly the periauricular area but some convenient location on the head. All sensors include evaluation boards compatible with Arduino microcontrollers, except the TMP112. Therefore, a custom solution was generated to be compatible with this initial prototype and periauricular measurements. All sensors were controlled with an Arduino Nano that included a Bluetooth 4.0 transceiver to wirelessly broadcast the signals. Power supply was implemented by means of a 3.7-V lithium-ion battery and a TTL port for manual event input or synchronization purposes was included.

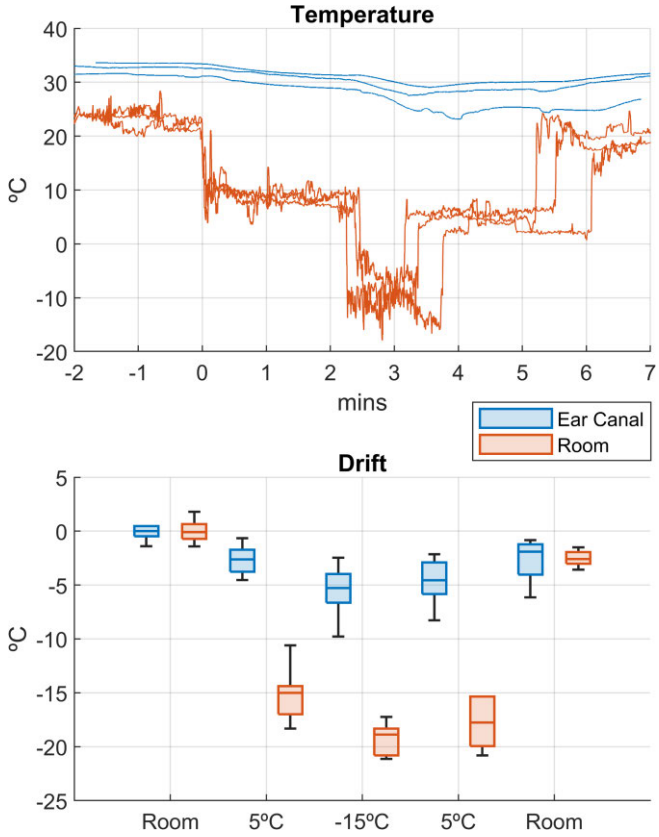

Fig. 11. (a) Example of temperature recordings in three representative volunteers during the temperature validation study with the TMP112 measuring the ear canal temperature (blue) and a TMP102 measuring ambient temperature (orange). (b) Temperature drift study for ear canal (blue) and ambient (orange) temperature through the different stages of the study. (c) Table summarizing the mean and SD of the drifts for each ambient temperature the volunteers are exposed to.

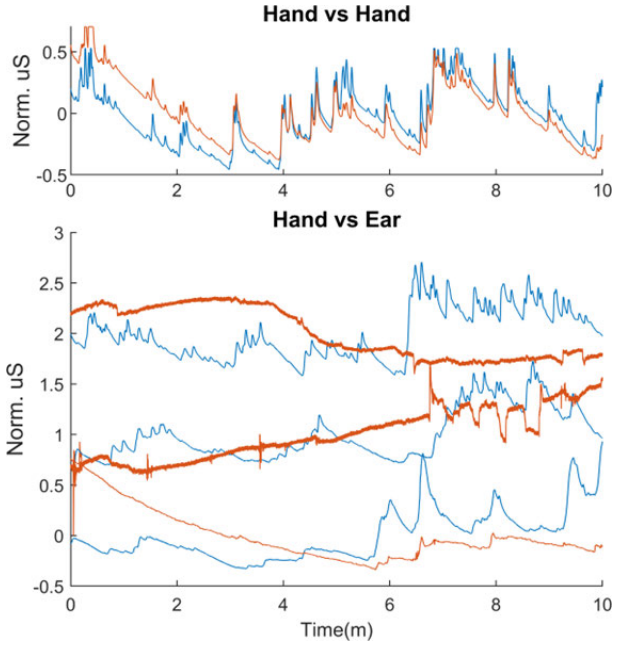

Fig. 12. Top panel: example of simultaneous GSR register in the two hands of a representative subject. Bottom panel: example of simultaneous recording of GSR in the hand (blue lines) and auricular area (orange) of three representative subjects (baseline of each of the recordings has been modified across subjects so recordings do not overlap). These are continuous recording going through the different Valsalva maneuvers.

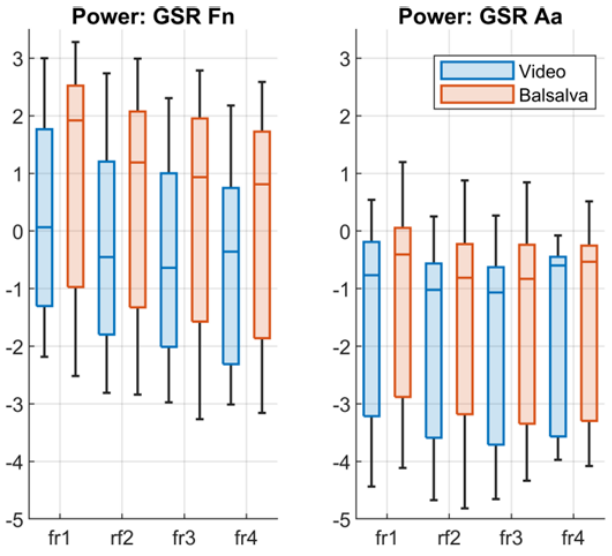

		GSR Finger				GSR Auricular Area			
		fr 1	fr 2	fr 3	fr 4	fr 1	fr 2	fr 3	fr 4
Video	Mn	0.13	-0.30	-0.59	-0.73	-1.57	-1.93	-1.99	-1.78
	STD	1.59	1.59	1.55	1.56	1.56	1.57	1.57	1.55
Bals.	Mn	0.89	0.44	0.18	-0.02	-1.27	-1.56	-1.65	-1.58
	STD	1.79	1.81	1.87	1.83	1.58	1.59	1.61	1.58
Significance		<0.001	<0.001	<0.001	<0.001	>0.05	0.05	0.08	>0.05

Fig. 13. Study of the power of the signal on the selected four frequency bands. The boxplots represent the power at the frequencies for the stimulation with the video (blue) and the Valsalva maneuver (orange): on the hand in the left and the auricular area on the left.

All mentioned components were attached (with Velcro or screws) to a head harness with an adjustable fastening system to fit with the different head sizes.

Finally, the setup was completed with the addition of an EEG signal recorded through a *BrainVision* system with electrodes placed in the periauricular area (see above). In the current version of the prototype, EEG data were not directly recorded by the Arduino Nano but synchronized with the *BrainVision* system by using the TTL port included. Thus, the setup demonstrates the feasibility of implementing the acquisition of the EEG, PPG, and core temperature from the periauricular area, together with accelerometry and room temperature signals simultaneously. Fig. 15 shows an example of one recording during the α-band modulation study. The EEG data coming from the EarSup electrode show a clear modulation of the α rhythm when the subject was asked to close his eyes and press the TTL marker. This marker was recorded and presented in the *BrainVision* system, and this picture has been filtered with a bandpass filter between 0.5 and 35 Hz, removing the high frequency and line noise and accentuating the α-band modulation on the EarSup electrode. The TTL channel shows the states of the volunteer: open (blue) and close (green) eyes. As can be seen, there is an increment on the activity of the EEG recording during the closed-eyes period, corresponding to ~10 Hz. The remaining parameters are correctly recorded: 1) the temperature shows the expected stable parameters; 2) the red and IR PPG signals show the

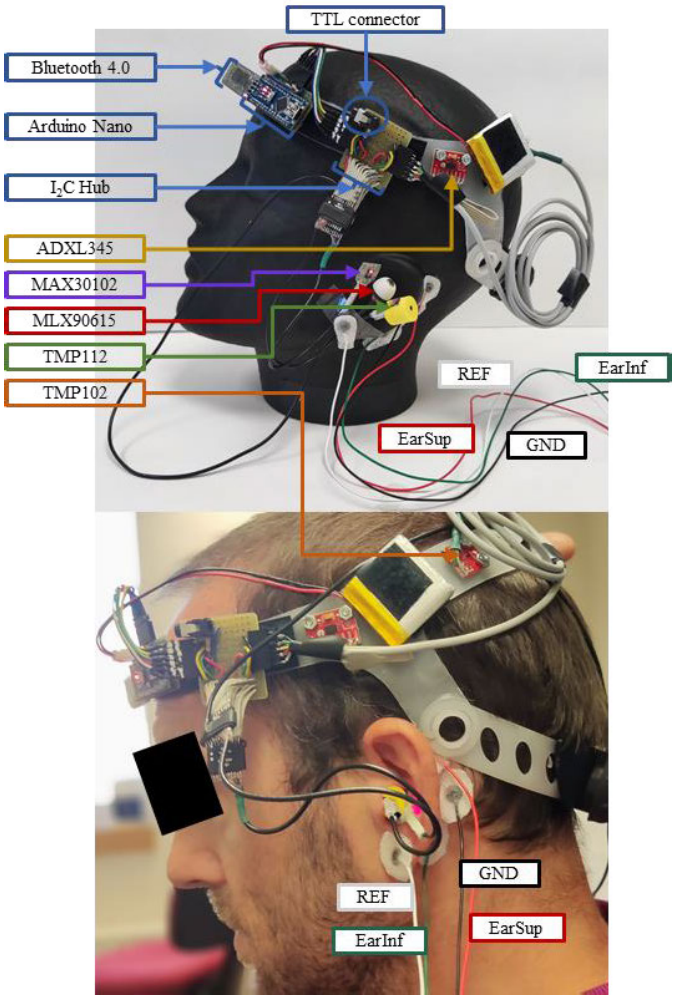

Fig. 14. Top panel: proof-of-concept prototype build around head harness including the following sensors: TMP102 (orange), TMP112 (green), ADXL345 (yellow), MAX30102 (purple), and MLX90615 (red). Blue indicated the remaining components for management, connection, and computing: Arduino Nano, lithium battery, Bluetooth 4.0, TTL connector, and I2C hub. The head sketches presented represent the placement of each component according to their color code. Bottom panel: photograph with all sensors on a human.

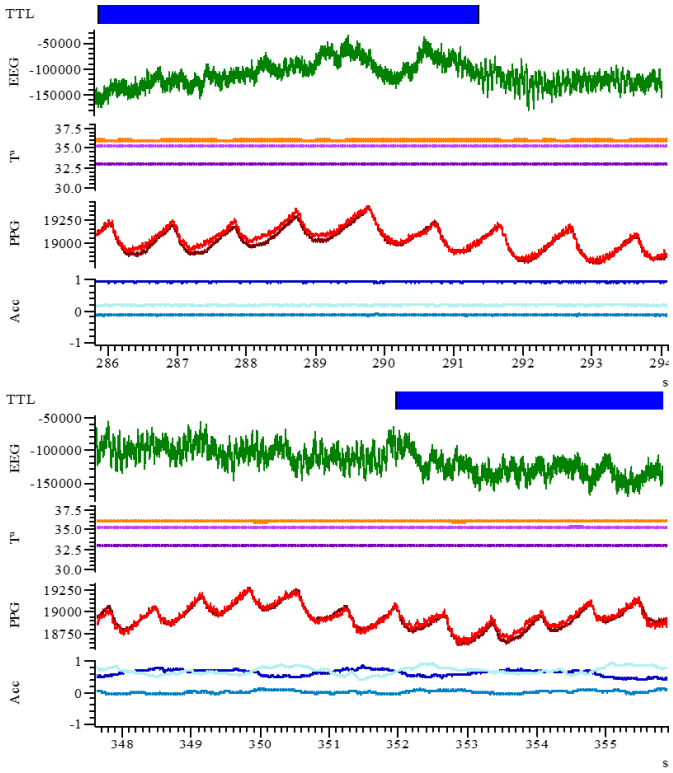

Fig. 15. Sample of the recordings obtained from two representative subjects with the presented proof-of-concept prototype and the *BrainVision* showing the four signal modalities and the TTL registers combined on a single recording.

waveform corresponding to each heartbeat synchronized for both signals; and 3) the acceleration shows stable acceleration measurements, despite some alterations due to subjects' movements to accommodate on the chair.

G. Body Area Network Wireless Connectivity

In order to gain insight in relation to the feasibility of employing BAN transceivers within the multimodal signal platform, coverage/capacity estimations have been obtained for Bluetooth Classic as well as for BLE. Different BAN topologies have been considered, following the path loss methodology described in [64], which considers the receiver position at chest or hip and the transmitter positions at chest, back, right wrist, and left wrist. The maximum data transmit power has been fixed to 10 dBm for both types of transceivers, considering that adaptive frequency hopping (AFH) is not active or that there are less than 15 channels available (in order to consider a more restrictive use case scenario; if AFH is active, then 20-dBm maximum transmission power is feasible). Receiver sensitivity thresholds have been set to -70 dBm for Bluetooth Classic and BLE 1M/2M, whereas for the case of BLE coded ($s = 2$), it has been set to -78 dBm, and for BLE coded ($s = 8$), it has been set to -85 dBm, following core Bluetooth specifications. The results are presented in Fig. 16, and as it can be seen, received power levels are in principle above sensitivity thresholds for all the link types under consideration. Further tests, however, are compulsory in order to evaluate wireless channel performance as a function of noise floor variations (due to variable interference conditions and considering different interference sources, i.e., intrasystem, intersystem, and external sources) and site-specific propagation conditions.

In order to assess the behavior of interbody/intrabody wireless links with the operating range of BT/BLE systems (a center operating frequency of 2.4 GHz), deterministic full-wave simulations have been performed with the aid of CST Microwave Studio. The human body voxel model "Gustav" has been employed, providing accurate frequency dispersive material characteristics. The CST Voxel Family is composed of different human body models, from eight persons of different gender, age, and stature. The biological data of all tissues present in human bodies are considered, as well as their electric properties, such as permittivity and conductivity [65]. In Fig. 17, the "Gustav" voxel model employed for the simulations described in this work can be seen. The numbered points represent the proposed location of the antennas for the

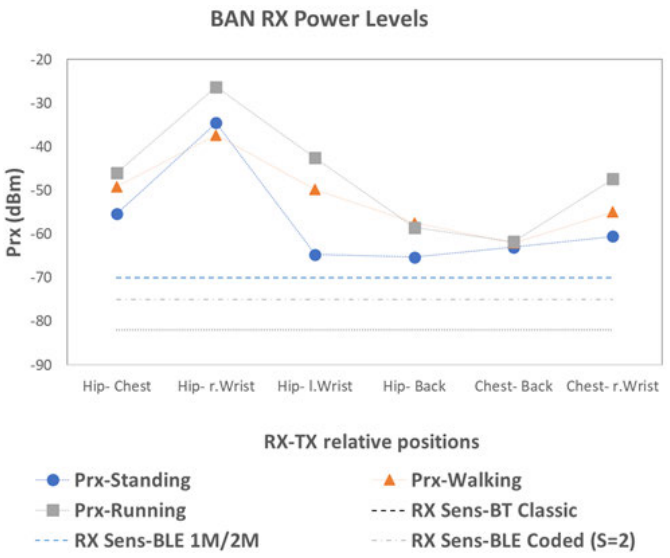

Fig. 16. Estimation of received power levels in relation to relative TX-RX positions within a body area network configuration. The values consider the use of Bluetooth as well as BLE transceivers.

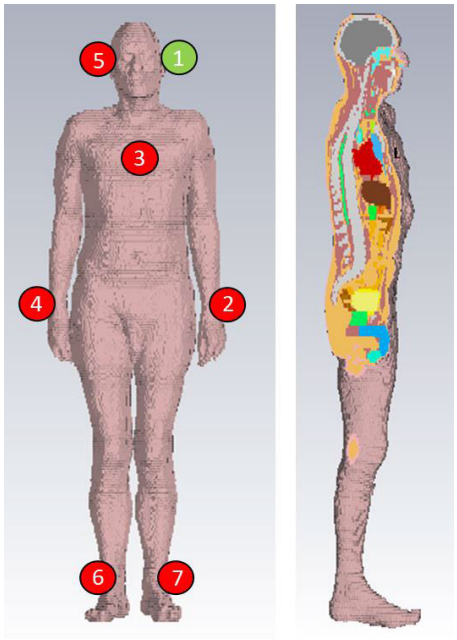

Fig. 17. Human body model employed for body area wireless link simulations. The numbered green dot cs the transmitter location, and the red dots represent the receiver locations.

wireless link analysis (the green dot represents the transmitter, emulating our sensor device, and the red ones represent the receivers). It is worth noting that, in this case, the transceiver location is flexible and, hence, can be located in a more convenient location (e.g., the transmitter in the periauricular area), compared to the previous wireless link model employed.

An antenna has been designed for the CST Microwave simulation, following the criteria of operating at 2.4 GHz and being as small as possible. Note that this antenna has been designed and simplified for the wireless link analysis, and the antenna integrated into the sensor device will be different after

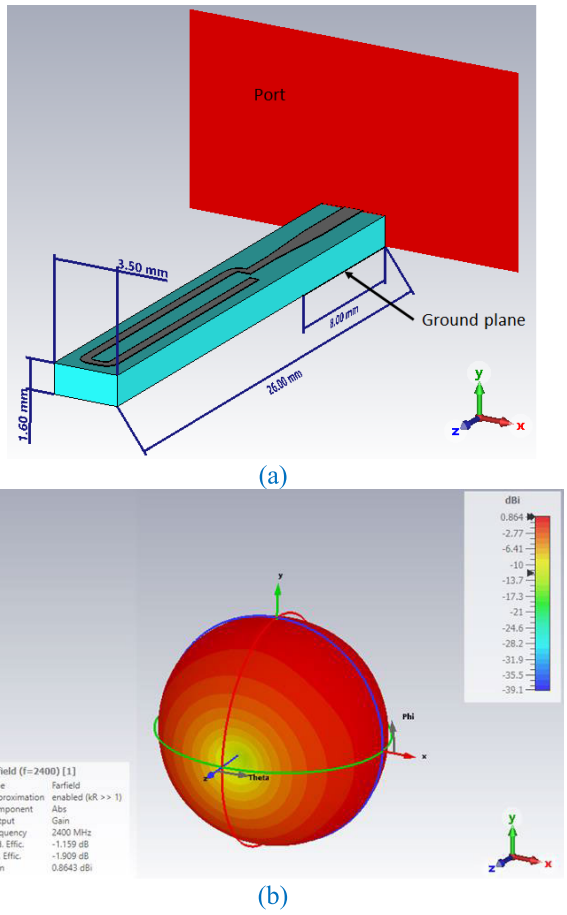

Fig. 18. (a) Antenna designed for the CST simulations. (b) Radiation pattern of the antenna.

considering the encapsulation of the whole device. Fig. 18 shows the designed antenna. The substrate is FR4 (dielectric constant = 4.37) and the metallic parts are copper.

This antenna has been included as transmitter and receiver at different points on the human body model in the simulation scenario presented in Fig. 17. Specifically, the transmitter has been located at the left ear, and the receivers have been located at the right ear, on the chest, both wrists, and both ankles. Fig. 19 presents the electric field distribution obtained by the CST Microwave Studio simulations. The employed human body allows obtaining propagation estimations in the air, in the body, and on the body.

The electric field propagation results and the inclusion of the antennas at the mentioned locations lead to the analysis of the wireless link in terms of the S_{21} parameter (i.e., transmission parameter), which represents the energy from the transmitter received by each receiver antenna (from the transmitter). The values of received power levels obtained for each one of the transceiver locations are given in Table I. The results show that received power levels in this case are lower, which is given, on one hand, in the difference in relation to the relative position of the transmitter–receiver pairs and, on the other hand, on a more precise consideration of human body impact as well as on the performance degradation of the realistic antenna model employed.

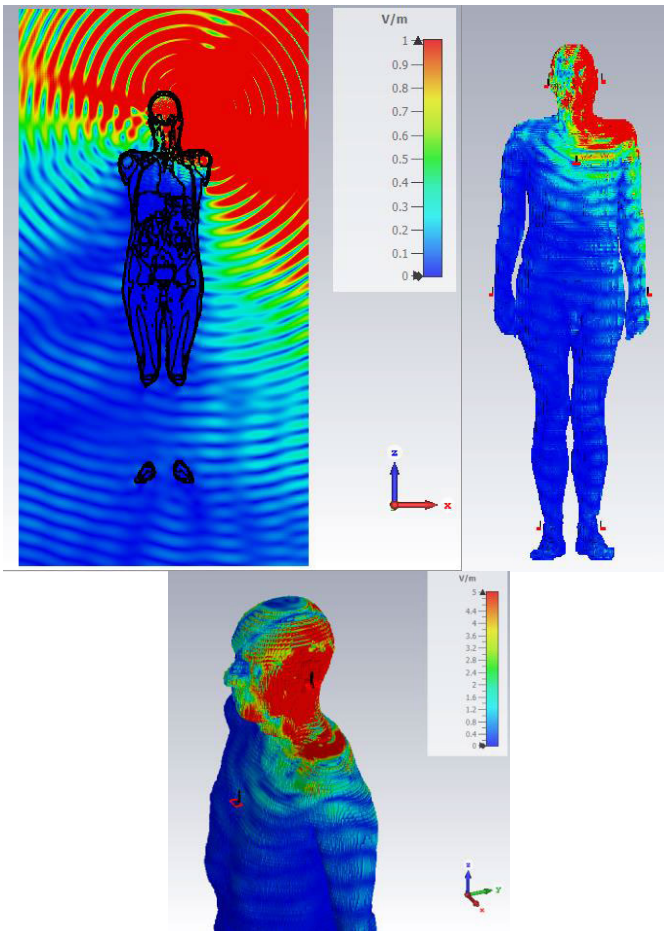

Fig. 19. CST Microwave Studio results: electric field distribution (both through the air, in and on the human body) generated by the transmitter, located at the left ear.

TABLE I
RECEIVER POWER LEVELS—FULL-WAVE RESULTS

Receiver Location (TX in Left Ear)	RX Power Level (dBm)
Left wrist	-69,53
Chest	-64,48
Right wrist	-97,93
Right ear	-91,16
Right ankle	-103,75
Left ankle	-81,64

As it can be seen, the interaction with the human body as well as with the surrounding environment results in degradation in quality, mainly by signal power loss (given by shadowing, diffraction, and scattering) and/or time-domain distortion, mainly given by multipath propagation. The topology of the human body as well as the existence of elements such as types of clothing can also be relevant, in terms of changes in losses as well as in terms of reflection and transmission coefficients given by the application of Fresnel's laws. In this sense, it is compulsory to perform the detailed wireless channel analysis, in order to fully consider the impact both on the human body as well as on the surrounding environment, aided by tools such as full-wave electromagnetic simulation and other approaches, such as deterministic bases modeling (e.g., geometric-stochastic models).

IV. CONCLUSION

The measurement of the purposed parameters has been fulfilled with mixed results. On one hand, the selected setup on the auricular area for PPG, acceleration temperature, and EEG shows an adequate behavior for the application purpose.

The ADX345 is capable of recording distinctive acceleration patterns corresponding to each activity tested, enabling the quantification of their similarities, and allowing future applications of motion classification. All temperature sensors provide adequate response to the different testing, being the TMP112 thermistor the selected sensor for both integration and validation studies given its behavior, robustness, and reduced dimensions. The drop-in temperature of 5.4 °C measured during the very cold environment exposure (where the user is exposed to 31.8 °C drop) shows that the area has the potential to provide adequate temperature measurements once the sensor placement and isolation are better approached. Nevertheless, this deviation of the measurements can be easily avoided by the use of protective clothing. In terms of PPG, the performed test showed that the behavior of this measurement on the auricular area is equivalent to its measurement on the gold standard on the finger. The HR and PTT studies showed the adequacy of the auricular area to acquire this signal modality. Moreover, the MAX30102 sensor can record the signal in the area of interest with enough quality to assess properly SpO_2- and HR-related parameters. In the case of EEG, the results show that it is possible to detect the α-modulation during an opened/closed eyes test as well as VEP and VSSRs. However, the equipment used does not admit integration with the rest of devices, and thus, a discrete device capable of similar (or better) recordings has to be selected.

In contrast to these four parameters, both ECG and GSR are discarded. Even with the restrictive electrode configuration, auricular area ECG records some cardiac activity with very low amplitude and inconsistent presence among subjects. However, as mentioned before, the PPG recordings show high signal quality and temporal coherence with the ECG being a great substitute for temporal characterization. In a similar manner, the GSR requires skin areas with enough separation between them to create some resistance to the applied current and active enough sweat glands during sympathetic arousal. Fortunately, multiple studies show that, despite being related to different physiological phenomena, both HRV and GSR can be used to assess the same type of emotional and sympathetic arousal. Thus, with the appropriate analysis tools, GSR can be substituted by the PPG. Nevertheless, GSR and ECG quality issues might be overcome with hardware modification, searching more adequate hardware or customized devices.

For the validation of four of the parameters, a wearable device has been developed integrating multiple temperature sensors, acceleration, and PPG devices. The current state of this prototype lacks a proper EEG integration to be considered complete. Despite this limitation being solved by synchronization through the TTL port, the volunteers wearing this system reported minor inconvenience in its use and sensor

placement on the auricular area. This and the quality of the recording, further validate the implementation and serve as a basis for future more ambitious implementations miniaturizing this device and upgrading its functionalities.

Even with the restrictiveness of the selected area for physiological signal recording, here, we have shown that it is feasible to obtain physiological data from the selected region. By doing so, we consider that it is possible to implement a wearable solution to determine the subject's state in an ergonomic and reliable way. In addition, body area network wireless connectivity analyses demonstrate the feasibility and limitations in terms of coverage/capacity conditions, as well as the detailed impact of human body presence intrabody/interbody links.

A device built for this purpose would not only be of great aid to epileptic patients and their relatives but would also be capable of detecting fever, motility disturbances, and low oxygen saturation; all of them very convenient for COVID-19 monitoring and early detection. Future work is also foreseen in the integration of wireless communication capabilities with BAN protocols as well as exploring further alternatives, such as low-power wide area network protocols, 5G NR FR1 (below 6-GHz bands, machine-type communications), or IEEE 802.11ah (sub-1-GHz IoT purpose specific connectivity). Moreover, security considerations within wearables must also be analyzed, playing a key role in overall user adoption [66].

The proposed system envisages a platform that is scalable, as a function of the microcontroller unit employed, as well as on the potential limitations given in terms of form factor as well as energy requirements. In this way and thinking on future evolutions, it is feasible to consider multiple alternatives, such as distributed computing nodes within the BAN, aggregated/multiplexed signal processing, and/or the increase in the unit size, which can be achieved supported by an external element that can be connected to the periauricular area. In this way, the system can span to tens of signals gathered. In terms of energy consumption, there are also multiple alternatives, also scalable in terms of energy consumption capabilities. This includes the use of elements, such as batteries and supercapacitors, with wireless power transfer mechanisms and hence the possibility of easily recharging the battery unit.

In relation to the system architecture, more extensive distributed computing schemes can be employed and are compatible with the proposed solution described in this work. Fog/cloud computing schemes can be indeed employed and can be beneficial for future system upgrades, in terms of data analysis/inference capabilities. The potential limitations of these network architectures are mainly derived in terms of latency, which for this specific application can have a lower impact for nonreal-time tasks, such as those aforementioned in relation to data analysis/processing/inference capabilities.

Acknowledgment

Guillermo M. Besné Villanueva, Julio Artieda González Granda, and Miguel Valencia Ustarroz are with the Biomedical Engineering Program, CIMA, Universidad de Navarra, 31080 Pamplona, Spain, and also with the Instituto de Investigación Sanitaria de Navarra (IdiSNA), 31008 Pamplona, Spain (e-mail: mvustarroz@unav.es).

Peio Lopez-Iturri, Jesús D. Trigo, and Luis Serrano-Arriezu are with the Institute of Smart Cities, Public University of Navarre, 31006 Pamplona, Spain, and also with the Instituto de Investigación Sanitaria de Navarra (IdiSNA), 31008 Pamplona, Spain.

Manuel Alegre Esteban is with the Biomedical Engineering Program, CIMA, Universidad de Navarra, 31080 Pamplona, Spain, and also with the Clínica Universidad de Navarra (CUN), 31008 Pamplona, Spain.

Francisco Falcone is with the Institute of Smart Cities, Public University of Navarre, 31006 Pamplona, Spain, also with the Instituto de Investigación Sanitaria de Navarra (IdiSNA), 31008 Pamplona, Spain, and also with the School of Engineering and Sciences, Tecnologico de Monterrey, Monterrey 64849, Mexico (e-mail: francisco.falcone@unavarra.es).

References

[1] M. W. J. Huygens et al., "Self-monitoring of health data by patients with a chronic disease: Does disease controllability matter?" *BMC Family Pract.*, vol. 18, no. 1, p. 40, Mar. 2017.

[2] M. W. J. Huygens, J. Vermeulen, I. C. S. Swinkels, R. D. Friele, O. C. P. van Schayck, and L. P. de Witte, "Expectations and needs of patients with a chronic disease toward self-management and eHealth for self-management purposes," *BMC Health Services Res.*, vol. 16, no. 1, p. 232, Dec. 2016.

[3] R. V. Milani, R. M. Bober, and C. J. Lavie, "The role of technology in chronic disease care," *Prog. Cardiovascular Diseases*, vol. 58, no. 6, pp. 579–583, 2016.

[4] D. V. Gunasekeran, "Technology and chronic disease management," *lancet. Diabetes Endocrinol.*, vol. 6, no. 2, p. 91, Feb. 2018.

[5] K. Lancaster et al., "The use and effects of electronic health tools for patient self-monitoring and reporting of outcomes following medication use: Systematic review," *J. Med. Internet Res.*, vol. 20, no. 12, p. e294, 2018. [Online]. Available: https//www.jmir.org/2018/12/

[6] J. M. Peake, G. Kerr, and J. P. Sullivan, "A critical review of consumer wearables, mobile applications, and equipment for providing biofeedback, monitoring stress, and sleep in physically active populations," *Frontiers Physiol.*, vol. 9, p. 743, Jun. 2018.

[7] M. Zhang, M. Luo, R. Nie, and Y. Zhang, "Technical attributes, health attribute, consumer attributes and their roles in adoption intention of healthcare wearable technology," *Int. J. Med. Informat.*, vol. 108, pp. 97–109, Dec. 2017.

[8] J.-M. Tsai, M.-J. Cheng, H.-H. Tsai, S.-W. Hung, and Y.-L. Chen, "Acceptance and resistance of telehealth: The perspective of dual-factor concepts in technology adoption," *Int. J. Inf. Manage.*, vol. 49, pp. 34–44, Dec. 2019.

[9] M. S. Rahman, "Does privacy matters when we are sick? An extended privacy calculus model for healthcare technology adoption behavior," in *Proc. 10th Int. Conf. Inf. Commun. Syst. (ICICS)*, Jun. 2019, pp. 41–46.

[10] L. Hogaboam and T. Daim, "Technology adoption potential of medical devices: The case of wearable sensor products for pervasive care in neurosurgery and orthopedics," *Health Policy Technol.*, vol. 7, no. 4, pp. 409–419, Dec. 2018.

[11] E. Bruno, P. F. Viana, M. R. Sperling, and M. P. Richardson, "Seizure detection at home: Do devices on the market match the needs of people living with epilepsy and their caregivers?" *Epilepsia*, vol. 61, no. S1, pp. S11–S24, Nov. 2020.

[12] T. Rukasha, S. I. Woolley, T. Kyriacou, and T. Collins, "Evaluation of wearable electronics for epilepsy: A systematic review," *Electronics*, vol. 9, no. 6, p. 968, Jun. 2020.

[13] C. E. Stafstrom and L. Carmant, "Seizures and epilepsy: An overview for neuroscientists," *Cold Spring Harbor Perspect. Med.*, vol. 5, no. 6, pp. a022426–a022426, Jun. 2015.

[14] O. Devinsky et al., "Epilepsy," *Nature Rev. Disease Primers*, vol. 4, no. 1, pp. 1–24, May 2018.

[15] L. Lagae, J. Irwin, E. Gibson, and A. Battersby, "Caregiver impact and health service use in high and low severity Dravet syndrome: A multinational cohort study," *Seizure*, vol. 65, pp. 72–79, Feb. 2019.

[16] J. Pimentel, "The epileptic multifactorial patient's burden. Review of the topic," *J. Epileptol.*, vol. 24, no. 2, pp. 167–172, Dec. 2016.

[17] G.-H. Kim, J. H. Byeon, S.-H. Eun, and B.-L. Eun, "Parents' subjective assessment of effects of antiepileptic drug discontinuation," *J. Epilepsy Res.*, vol. 5, no. 1, pp. 9–12, Jun. 2015.

[18] M. Teplan, "Fundamentals of EEG measurement," *Meas. Sci. Rev.*, vol. 2, no. 2, pp. 1–10, 2002.

[19] S. Noachtar and J. Rémi, "The role of EEG in epilepsy: A critical review," *Epilepsy Behav.*, vol. 15, no. 1, pp. 22–33, May 2009.

[20] K. B. Mikkelsen, S. L. Kappel, D. P. Mandic, and P. Kidmose, "EEG recorded from the ear: Characterizing the ear-EEG method," *Frontiers Neurosci.*, vol. 9, pp. 1–8, Nov. 2015.

[21] A. Paul, S. R. Deiss, D. Tourtelotte, M. Kleffner, T. Zhang, and G. Cauwenberghs, "Electrode-skin impedance characterization of in-ear electrophysiology accounting for cerumen and electrodermal response," in *Proc. 9th Int. IEEE/EMBS Conf. Neural Eng. (NER)*, Mar. 2019, pp. 855–858.

[22] M. Eickenscheidt, P. Schäfer, Y. Baslan, C. Schwarz, and T. Stieglitz, "Highly porous platinum electrodes for dry ear-EEG measurements," *Sensors*, vol. 20, no. 11, pp. 1–12, Jun. 2020.

[23] C. Athavipach, S. Pan-Ngum, and P. Israsena, "A wearable in-ear EEG device for emotion monitoring," *Sensors*, vol. 19, no. 18, p. 4014, Sep. 2019.

[24] V. Goverdovsky et al., "Hearables: Multimodal physiological in-ear sensing," *Sci. Rep.*, vol. 7, no. 1, pp. 1–10, Jul. 2017.

[25] M. G. Bleichner and S. Debener, "Concealed, unobtrusive ear-centered EEG acquisition: CEEGrids for transparent EEG," *Frontiers Hum. Neurosci.*, vol. 11, p. 163, Apr. 2017.

[26] Y. Gu et al., "Comparison between scalp EEG and behind-the-ear EEG for development of a wearable seizure detection system for patients with focal epilepsy," *Sensors*, vol. 18, no. 2, p. 29, Dec. 2017.

[27] I. C. Zibrandtsen, P. Kidmose, C. B. Christensen, and T. W. Kjaer, "Ear-EEG detects ictal and interictal abnormalities in focal and generalized epilepsy—A comparison with scalp EEG monitoring," *Clin. Neurophysiol.*, vol. 128, no. 12, pp. 2454–2461, Dec. 2017.

[28] S. M. Rissanen et al., "Wearable monitoring of positive and negative myoclonus in progressive myoclonic epilepsy type 1," *Clin. Neurophysiol.*, vol. 132, no. 10, pp. 2464–2472, Oct. 2021.

[29] M. Ghamari, "A review on wearable photoplethysmography sensors and their potential future applications in health care," *Int. J. Biosensors Bioelectron.*, vol. 4, no. 4, pp. 195–202, 2018.

[30] G.-J. Horng and K.-H. Chen, "The smart fall detection mechanism for healthcare under free-living conditions," *Wireless Pers. Commun.*, vol. 118, no. 1, pp. 715–753, Jan. 2021.

[31] J. P. Wolff, F. Grützmacher, A. Wellnitz, and C. Haubelt, "Activity recognition using head Worn inertial sensors," in *Proc. 5th Int. Workshop Sensor-based Activity Recognit. Interact.*, Sep. 2018, pp. 1–7.

[32] M. Alghatrif and J. Lindsay, "A brief review: History to understand fundamentals of electrocardiography," *J. Community Hospital Internal Med. Perspect.*, vol. 2, no. 1, p. 14383, Apr. 2012, doi: 10.3402/JCHIMP.V2I1.14383.

[33] K. Khunti, "Accurate interpretation of the 12-lead ECG electrode placement: A systematic review," *Health Educ. J.*, vol. 73, no. 5, pp. 610–623, Sep. 2014.

[34] L. Billeci, A. Tonacci, D. Marino, L. Insana, G. Vatti, and M. Varanini, "A machine learning approach for epileptic seizure prediction and early intervention," in *Converging Clinical and Engineering Research on Neurorehabilitation III* (Biosystems & Biorobotics), vol. 21. Cham, Switzerland: Springer, 2019, pp. 972–976.

[35] A. van Westrhenen, T. De Cooman, R. H. C. Lazeron, S. Van Huffel, and R. D. Thijs, "Ictal autonomic changes as a tool for seizure detection: A systematic review," *Clin. Autonomic Res.*, vol. 29, no. 2, pp. 161–181, Apr. 2019.

[36] G. Giannakakis, M. Tsiknakis, and P. Vorgia, "Focal epileptic seizures anticipation based on patterns of heart rate variability parameters," *Comput. Methods Programs Biomed.*, vol. 178, pp. 123–133, Sep. 2019.

[37] Y. Sun and N. Thakor, "Photoplethysmography revisited: From contact to noncontact, from point to imaging," *IEEE Trans. Biomed. Eng.*, vol. 63, no. 3, pp. 463–477, Mar. 2016.

[38] J. Allen, "Photoplethysmography and its application in clinical physiological measurement," *Physiolog. Meas.*, vol. 28, no. 3, pp. R1–R39, Mar. 2007.

[39] Y. Maeda, M. Sekine, and T. Tamura, "Relationship between measurement site and motion artifacts in wearable reflected photoplethysmography," *J. Med. Syst.*, vol. 35, no. 5, pp. 969–976, May 2010.

[40] S. Bagha, S. Hills, P. Bhubaneswar, and L. Shaw, "A real time analysis of PPG signal for measurement of SpO_2 and pulse rate," *Int. J. Comput. Appl.*, vol. 36, no. 11, pp. 40–50, 2011.

[41] R. J. Thomas, J. E. Mietus, C.-K. Peng, and A. L. Goldberger, "An electrocardiogram-based technique to assess cardiopulmonary coupling during sleep," *Sleep*, vol. 28, no. 9, pp. 1151–1161, Sep. 2005.

[42] C. Varon, K. Jansen, L. Lagae, L. Faes, and S. Van Huffel, "Transient behavior of cardiorespiratory interactions towards the onset of epileptic seizures," *Comput. Cardiol.*, vol. 41, pp. 917–920, Jan. 2014.

[43] C. Varon et al., "Interictal cardiorespiratory variability in temporal lobe and absence epilepsy in childhood," *Physiolog. Meas.*, vol. 36, no. 4, pp. 845–856, Apr. 2015.

[44] S. Passler, N. Müller, and V. Senner, "In-ear pulse rate measurement: A valid alternative to heart rate derived from electrocardiography?" *Sensors*, vol. 19, no. 17, p. 3641, Aug. 2019.

[45] V. Bach, F. Telliez, and J. P. Libert, "The interaction between sleep and thermoregulation in adults and neonates," *Sleep Med. Rev.*, vol. 6, no. 6, pp. 481–492, Dec. 2002.

[46] A. K. Leung, K. L. Hon, and T. N. Leung, "Febrile seizures: An overview," *Drugs Context*, vol. 7, pp. 1–12, Jul. 2018.

[47] M. Sund-Levander, C. Forsberg, and L. K. Wahren, "Normal oral, rectal, tympanic and axillary body temperature in adult men and women: A systematic literature review," *Scandin. J. Caring Sci.*, vol. 16, no. 2, pp. 122–128, Jun. 2002.

[48] R. Norman, L. Mendolicchio, and C. Mordeniz, "Galvanic skin response & its neurological correlates," *J. Consciousness Explor. Res.*, vol. 7, no. 7, pp. 553–572, 2016.

[49] R. L. Bailey, "Electrodermal activity (EDA)," in *The International Encyclopedia of Communication Research Method*. Chicago, IL, USA: Wiley, 2017, pp. 1–15.

[50] R. Martinez, A. Salazar-Ramirez, A. Arruti, E. Irigoyen, J. I. Martin, and J. Muguerza, "A self-paced relaxation response detection system based on galvanic skin response analysis," *IEEE Access*, vol. 7, pp. 43730–43741, 2019.

[51] M.-Z. Poh et al., "Convulsive seizure detection using a wrist-worn electrodermal activity and accelerometry biosensor," *Epilepsia*, vol. 53, no. 5, pp. e93–e97, May 2012.

[52] R. W. Picard et al., "Wrist sensor reveals sympathetic hyperactivity and hypoventilation before probable SUDEP," *Neurology*, vol. 89, no. 6, pp. 633–635, Aug. 2017.

[53] M. van Dooren, J. J. G.-J. de Vries, and J. H. Janssen, "Emotional sweating across the body: Comparing 16 different skin conductance measurement locations," *Physiol. Behav.*, vol. 106, no. 2, pp. 298–304, May 2012.

[54] C. J. Smith and G. Havenith, "Body mapping of sweating patterns in male athletes in mild exercise-induced hyperthermia," *Eur. J. Appl. Physiol.*, vol. 111, no. 7, pp. 1391–1404, Jul. 2011.

[55] S. L. Kappel, M. L. Rank, H. O. Toft, M. Andersen, and P. Kidmose, "Dry-contact electrode ear-EEG," *IEEE Trans. Biomed. Eng.*, vol. 66, no. 1, pp. 150–158, Jan. 2019.

[56] P. Stoica and R. Moses, *Spectral Analysis Of Signals*. Upper Saddle River, NJ, USA: Prentice-Hall, 2005.

[57] B. Porat, *Digital Processing of Random Signals: Theory and Methods*, 2008.

[58] D. J. Creel, "Visually evoked potentials," *Handb. Clin. Neurol.*, vol. 160, pp. 501–522, Jan. 2019.

[59] M. Müller, "Dynamic time warping," in *Information Retrieval for Music and Motion*. Berlin, Germany: Springer, 2007, pp. 69–84.

[60] R. Muscillo, S. Conforto, M. Schmid, P. Caselli, and T. D'Alessio, "Classification of motor activities through derivative dynamic time warping applied on accelerometer data," in *Proc. 29th Annu. Int. Conf. IEEE Eng. Med. Biol. Soc.*, Aug. 2007, pp. 4930–4933.

[61] N. Ö. Doğan, "Bland-Altman analysis: A paradigm to understand correlation and agreement," *Turkish J. Emergency Med.*, vol. 18, no. 4, pp. 139–141, Dec. 2018.

[62] R. Zangróniz, A. Martínez-Rodrigo, J. M. Pastor, M. T. López, and A. Fernández-Caballero, "Electrodermal activity sensor for classification of calm/distress condition," *Sensors*, vol. 17, no. 10, pp. 1–14, 2017.

[63] D. B. Smith, D. Miniutti, T. A. Lamahewa, and L. W. Hanlen, "Propagation models for body-area networks: A survey and new outlook," *IEEE Antennas Propag. Mag.*, vol. 55, no. 5, pp. 97–117, Oct. 2013.

[64] D. Smith, D. Miniutti, L. Hanlen, A. Zhang, D. Lewis, and D. Rodda, *Power Delay Profiles for Dynamic Narrowband Body Area Network Channels*, document 802.15-09-0187-01-0006, Mar. 2009.

[65] *CST Human Body Model*. Accessed: Nov. 25, 2022. [Online]. Available: https://space.mit.edu/RADIO/CST_online/mergedProjects/3D/common_tools/common_tools_biomodels.htm

[66] H. Amintoosi et al., "Secure and authenticated data access and sharing model for smart wearable systems," *IEEE Internet Things J.*, vol. 9, no. 7, pp. 5368–5379, Apr. 2022, doi: 10.1109/JIOT.2021.3109274.

Guillermo M. Besné Villanueva received the B.E. and M.E. degrees in biomedical engineering from TECNUN, University of Navarra, Donostia-San Sebastián, Spain, in 2015 and 2017, respectively, and the Ph.D. degree in biomedicine and applied medicine from the Program of Neurosciences of CIMA, University of Navarra, Pamplona, Spain, in 2022, under the supervision of M. Valencia Ustarroz.

His research interests include biomedical and healthcare device development, patient monitoring, and data science applications on physiological recordings with special interest in neuropathologies, such as epilepsy.

Peio Lopez-Iturri received the bachelor's degree in telecommunications engineering, the master's degree in communications, and the Ph.D. degree in communication engineering from the Public University of Navarre (UPNA), Pamplona, Spain, in 2011, 2012, and 2017, respectively.

He has worked in 18 different public and privately funded research projects. In 2019, he partly worked as a Researcher for Tafco Metawireless, Ansoáin, Spain. He has over 200 contributions in indexed international journals, book chapters, and conference contributions. He is affiliated with the Institute for Smart Cities (ISC), UPNA. His research interests include radio propagation, wireless sensor networks, electromagnetic dosimetry, modeling of radio interference sources, mobile radio systems, wireless power transfer, IoT networks and devices, 5G communication systems, and electromagnetic compatibility (EMC)/electromagnetic interference (EMI).

Dr. Lopez-Iturri was a recipient of the ECSA 2014 Best Paper Award, the IISA 2015 Best Paper Award, the ISSI 2019 Best Paper Award, and the EAI Industrial IoT 2020 Best Paper Award. He received the 2018 Best Spanish Ph.D. Thesis in Smart Cities in CAEPIA 2018 (3rd prize), sponsored by the Spanish network on research for Smart Cities CI-RTI and Sensors.

Manuel Alegre Esteban received the bachelor's and Ph.D. degrees in medicine and surgery from the University of Navarra, Pamplona, Spain, in 1994 and 2002, respectively.

He is a Specialist in Neurology and Clinical Neurophysiology and currently heads the Neurophysiology Service of the Clínica Universidad de Navarra, Pamplona. His main field of research interest is brain oscillatory activity in relation to physiological motor control and its alterations (movement disorders). His other fields of interest are the physiology of the auditory pathway and the relationship between oscillatory activity and cognition.

Dr. Alegre Esteban has received several awards, including the Extraordinary Degree Award in 1994 and the Extraordinary Doctorate Award in 2002. He belongs to the Spanish Society of Neurophysiology, Spanish Society of Neurology, Movement Disorders Society, and Society for Neuroscience. He has been member of the Editorial Committee of *Clinical Neurophysiology* and Editorial Assistant of *Movement Disorders*.

Julio Artieda González Granda received the bachelor's degree in medicine and Ph.D. degree in medicine from the University of Navarra (UNAV), Pamplona, Spain, in 1978 and 1979, respectively.

He is a specialist in neurophysiology and neurology. He completed his studies at the Hôpital de Sainte Anne, Université Cochine-Port Royal, Paris, France. He is currently an Emeritus Professor of Neurology at UNAV. He has been Director of the Neurology Department and Head of the Clinical Neurophysiology Service, Clínica Universidad de Navarra, (CUN), Pamplona; Director of the Doctoral Program in Neuroscience and Cognition and Coordinator of the Neuroscience Area of the Center for Applied Medical Research (CIMA) and Navarra Health Research Institute (IdisNA), Pamplona. He is the author of more than 150 peer-reviewed publications and 20 books. In recent years, he has been interested in the role of brain oscillatory activity in information processing at the brain level and its role in different neurological diseases, such as Parkinson's disease or psychiatric diseases such as schizophrenia.

Jesús D. Trigo was born in Zaragoza, Spain, in 1981. He received the M.S. degree in telecommunication engineering and the Ph.D. (Hons.) degree from the University of Zaragoza, Zaragoza, Spain, in 2005 and 2011, respectively.

He is currently an Assistant Professor with the Department of Electrical, Electronic and Communications Engineering, Public University of Navarre, Pamplona, Spain. He has undergone research stages at the Biomedical Informatics Laboratory, Foundation for Research and Technology-Hellas, Heraklion, Crete, Greece, and the Institute of Medical Biometry and Informatics, Heidelberg University, Heidelberg, Germany. He is the author of 17 articles, five book chapters, and over 50 publications in national and international conference proceedings. He has participated in over ten research projects with both public and private funding and has advised one Ph.D. thesis. His research interests include eHealth applications and architectures, biomedical informatics or medical device interoperability, and standardization among others.

Luis Serrano-Arriezu (Senior Member, IEEE) was born in Andosilla, Spain, in 1966. He received the M.Sc. degree in physics from the University of Zaragoza, Zaragoza, Spain, in 1989, and the Ph.D. degree in electrical engineering from the Public University of Navarra, Pamplona, Spain, in 1995.

He has been involved in the design and manufacture of medical devices for vital sign measurements (BP, SpO_2, optical, and bioelectronics), the development of interoperability standards for medical devices, strategies for the deployment of new ICT-based electronic health services, the Internet of Medical Things (IoMT), startup entrepreneurship, as well as the elaboration of study plans (bachelor, master, and Ph.D.) in this field. During this time, he has published more than 90 articles in indexed international journals as well as in national and international congresses, several book chapters, as well as the publication of a national patent. He has also managed numerous research projects, collaborative projects, and technology transfer with private companies, as well as innovation and development contracts and six doctoral theses.

Francisco Falcone (Senior Member, IEEE) received the degree in telecommunication engineering and the Ph.D. degree in communication engineering from the Public University of Navarre (UPNA), Pamplona, Spain, in 1999 and 2005, respectively.

From 1999 to 2000, he was a Microwave Network Engineer at Siemens-Italtel, Málaga, Spain. From 2000 to 2008, he was a Mobile Access Network Engineer at Telefónica Móviles, Pamplona. In 2009, he co-founded Tafco Metawireless, a spin-off of UPNA (with EIBT national label), of which he was its first manager. In parallel, from 2003 to 2009, he was an Assistant Lecturer with the Department of Electrical and Electronic Engineering, UPNA, where he became an Associate Professor in June 2009. From 2011 to 2012, he was a Secretary at the Department of Electrical, Electronic and Communication Engineering, UPNA, where he was the Head of the Department of Electrical, Electronic and Communication Engineering from January 2012 to July 2018 and from July 2019 to November 2021. In 2018, he was a Visiting Professor at the Kuwait College of Science and Technology, Doha, Kuwait, for three months. He has also been with the Smart Cities Institute, Public University of Navarra, a multidisciplinary research institute with over 100 researchers, being the Head of the Institute, since May 2021, working on contextual and interactive environments solutions, through the integration of heterogeneous wireless communications networks, based on HetNet and the IoT. Since June 2022, he has been a Distinguished Visiting Professor with the Telecommunications School of Engineering and Science, Tecnologico de Monterrey, Monterrey, Mexico. Since September 2022, he has also been a Full Professor with the Department of Electrical, Electronic and Communication Engineering, UPNA. He has over 600 contributions in indexed international journals, book chapters, and conference contributions. His research interests include computational electromagnetics applied to the analysis of complex electromagnetic scenarios, with a focus on the analysis, design, and implementation of heterogeneous wireless networks to enable context-aware environments.

Dr. Falcone received several research awards, such as the CST Best Paper Award in 2003 and 2005, the Prize of the Official Association of Telecommunications Engineers for the Best Doctoral Thesis in 2005, the UPNA Ph.D. Award in Experimental Sciences from 2004 to 2006, the 1st Prize Juan López de Peñalver to the Best Young Researcher in 2010, the Real Academia de Ingeniería de España, the XII Talgo Foundation Award for Technological Innovation with the proposal "Implementation of an Environment for the Railway Ecosystem," the ECSA-2 Best Paper Award in 2015, the Best Paper Award IISA in 2015, the ECSA Award-3 Best Paper Award in 2016, the ECSA-4 Best Paper Award in 2018, the Best Paper Award ISSI in 2019, and the IIoT 2020 Best Paper Award.

Miguel Valencia Ustarroz received the B.E. degree in telecommunications engineering from the Public University of Navarra (UPNA), Pamplona, Spain, in 2001, followed by an expert in biomedical engineering, and the Ph.D. degree in applied physics and mathematics from UPNA in 2006.

From 2003 to 2006, he participated in the establishment of the Laboratory of Clinic Neurophysiology, Center for Applied Medical Research (CIMA), during his Ph.D. From 2007 to 2009, he worked with CNRS on the LENA Laboratory located at the Pitié-Salpêtrière Hospital, Paris, France. Afterward, he was reincorporated on CIMA as a Junior Researcher and now leads the Physiological Monitoring and Control Laboratory, CIMA. He is the author of over 50 publications, two book chapters, and 120 scientific communications.

Dr. Valencia Ustarroz is a member of the Spanish Society for Neuroscience and the Spanish Society of Biomedical Engineering.